



1 Primary and secondary emissions from a modern fleet of city buses

2 Liyuan Zhou^{1,2#}, Qianyun Liu^{2,a#}, Christian M. Salvador^{3,b}, Michael Le Breton^{3,c}, Mattias Hallquist³, Jian
3 Zhen Yu⁴ and Chak K. Chan^{1,2*}, Åsa M. Hallquist^{5*}

4

5 ¹ Division of Physical Sciences and Engineering, King Abdullah University of Science and Technology, Thuwal, Saudi Arabia

6 ² School of Energy and Environment, City University of Hong Kong, Hong Kong SAR, China

7 ³ Department of Chemistry and Molecular Biology, University of Gothenburg, Gothenburg, Sweden

8 ⁴ Division of Environment and Sustainability, Hong Kong University of Science and Technology, Hong Kong, China

9 ⁵ IVL Swedish Environmental Research Institute, Gothenburg, Sweden

10 ^anow at: RELX Science Center, Shenzhen RELX Tech. Co., Ltd., Shenzhen, China

11 ^bnow at: Environmental Sciences Division, Oak Ridge National Laboratory, Oak Ridge, TN 37830, USA

12 ^cnow at: FEV Sverige AB, Gothenburg, Sweden

13

14

15 #The authors contribute equally.

16 *Correspondence to:* Åsa M Hallquist (asa.hallquist@ivl.se); Chak K. Chan (chak.chan@kaust.edu.sa)

17

18 **Abstract.** The potential impact of transitioning from conventional fossil fuel to a non-fossil fuel vehicle fleet was investigated
19 by measuring primary emissions via extractive sampling of bus plumes and assessing secondary mass formation using a
20 Gothenburg Potential Aerosol Mass (Go:PAM) reactor from 76 in-use transit buses. Online chemical characterization of
21 gaseous and particle emissions from these buses was conducted using a chemical ionization mass spectrometry (CIMS) with
22 acetate as the reagent ion, coupled with a filter inlet for gases and aerosols (FIGAERO). A significant reduction (48-98%) in
23 fresh particle emissions was observed in buses utilizing compressed natural gas (CNG), biodiesels like rapeseed methyl ester
24 (RME) and hydrotreated vegetable oil (HVO), as well as hybrid-electric HVO (HVO_{HEV}), compared to diesel (DSL) buses.
25 However, secondary particle formation from photooxidation of emissions was substantial across all fuel types. The median
26 ratio of particle mass emission factors of aged to fresh emissions increased in the following order: DSL buses at 4.0, HVO
27 buses at 6.7, HVO_{HEV} buses at 10.5, RME buses at 10.8, and CNG buses at 84. Of the compounds that can be identified by
28 CIMS, fresh gaseous emissions from all Euro V/EEV buses, regardless of fuel type, were dominated by nitrogen-containing
29 compounds such as nitrous acid (HONO), nitric acid (HNO₃), and isocyanic acid (HNCO), alongside small monoacids (C₁-
30 C₃). Notably, nitrogen-containing compounds were significantly reduced in Euro VI buses equipped with more advanced
31 emission control technologies. Secondary gaseous organic acids correlated strongly with gaseous HNO₃ signals (R²= 0.85-
32 0.99) in Go:PAM, but their moderate to weak correlations with post-photooxidation secondary particle mass suggest they are
33 not reliable tracers for secondary organic aerosol formation from bus exhaust. Our study highlights that non-regulated
34 compounds and secondary pollutant formation, not currently addressed in legislation, are crucial considerations in the
35 evaluation of environmental impacts of future fuel and engine technology shifts.



36 1. Introduction

37 Air pollution remains a critical global issue, posing significant threats to both human health and the environment. Despite
38 substantial progress in reducing emissions from major sources like industry, energy production, households, transportation,
39 and agriculture, the worldwide achievement of air quality targets continues to be a daunting challenge. Notably, the road
40 transport sector, particularly in urban environments, significantly contributes to the emissions of nitrogen oxides (NO_x) and
41 particulate matter (PM), impacting the health of individuals in densely populated regions. In tandem with these concerns,
42 efforts to combat climate change have spurred an increase in the adoption of renewable energy sources within the transportation
43 sector. Biodiesel has risen as the most prevalent renewable fuel, followed by biogas and ED95 ethanol (Guerreiro et al., 2014).
44 Moreover, numerous cities are progressively integrating hybrid-electric and electric vehicles into their public transport fleets,
45 aiming to reduce emissions.

46

47 Emissions from vehicles, especially buses, exhibit considerable variability. They are influenced by fuel type, engine design,
48 operational conditions, emission after-treatment technologies and maintenance (Zhao et al., 2018; Watne et al., 2018; Pirjola
49 et al., 2016; Liu et al., 2019a; Zhou et al., 2020). While diesel (DSL) buses are common, there is an increasing trend towards
50 the use of alternative fuels such as compressed natural gas (CNG), rapeseed methyl ester (RME), and hydrotreated vegetable
51 oil (HVO). These alternative fuels offer several benefits, including reduced PM emissions, particularly soot, and lower levels
52 of carbon monoxide (CO) and total hydrocarbons (THC) (Pflaum et al., 2010; Hassaneen et al., 2012; Liu et al., 2019a).
53 However, the efficacy of RME and HVO in diminishing NO_x emissions can be inconsistent (Pirjola et al., 2016; Liu et al.,
54 2019a); and CNG buses exhibit considerable variability in particle number (PN) emissions (Watne et al., 2018). In Sweden,
55 approximately 23% of the fuel mix of the transport sector in 2020 comprised renewable fuels, with HVO accounting for over
56 half of this proportion (Vourliotakis and Platsakis, 2022; Energimyndigheten, 2021). Emission control strategies, such as
57 aftertreatment systems including diesel particulate filters (DPFs) and selective catalytic reduction (SCR) systems, have been
58 implemented to mitigate pollutant emissions from vehicles. These systems have shown significant efficacy in reducing PM
59 and NO_x emissions respectively, though their performance can vary under different operational conditions.

60

61 Accurately determining vehicle emission factors (EFs) is essential for developing and implementing effective air quality
62 policies (Fitzmaurice and Cohen, 2022). Various methodologies, including testing cycles, on-road chasing, and portable
63 emission measurement systems (PEMS), have been employed to measure vehicle emissions (Kwak et al., 2014; Jezek et al.,
64 2015; Pirjola et al., 2016). Roadside or near-road measurements of on-road vehicle emissions provide a larger sample size in
65 a shorter timeframe, which is especially relevant for estimating the exposure of pedestrians and bus passengers. In a prior
66 study, we reported EFs for general air pollutants such as PM, NO_x, CO, and THC from individual buses in an in-use bus fleet,
67 based on stop-and-go measurements at a bus stop in Gothenburg, Sweden (Liu et al., 2019a). Our findings indicated that



68 hybrid buses, when using their combustion engines to accelerate from a standstill at bus stops, tended to emit higher particle
69 numbers (PN) than traditional DSL buses, likely due to their relatively smaller engines.

70

71 Primary emissions are not the only way in which engine emissions impact air quality. Emissions from engine exhaust can
72 contribute to secondary particles through oxidation of gas-phase species, primarily via functionalization reactions, yielding
73 lower-volatility products (Hallquist et al., 2009; Kroll et al., 2009). Laboratory studies have demonstrated that the amount of
74 secondary organic aerosols (SOA) produced from diluted vehicle exhaust frequently surpasses that of primary organic aerosols
75 (POA) within less than one day of atmospheric equivalent aging (Nordin et al., 2013; Platt et al., 2013; Gordon et al., 2014b;
76 Liu et al., 2015; Chirico et al., 2010). In addition, primary emissions may also be oxidized to higher-volatility products via
77 fragmentation reactions. Engine exhaust is a recognized primary source of organic acids in the atmosphere (Friedman et al.,
78 2017), and the oxidation of hydrocarbons from the exhaust by hydroxyl radicals (OH) results in a diverse array of products
79 with numerous functional groups, including carboxylic acids ($-\text{COOH}$) (Yao et al., 2002). However, the secondary production
80 of organic acid from engine exhaust remains poorly characterized; and it may significantly contribute to the overall organic
81 acid budget and help explain discrepancies between models and measurements (Millet et al., 2015; Yuan et al., 2015; Paulot
82 et al., 2011). Recent development of analytical techniques has enabled tools for simultaneous online measurements of gas and
83 particle phase species at a high time resolution by utilizing a high-resolution time-of-flight chemical ionization mass
84 spectrometry (HR-ToF-CIMS) coupled with a filter inlet for gases and aerosols (FIGAERO) (Le Breton et al., 2019; Friedman
85 et al., 2017; Lopez-Hilfiker et al., 2014; Zhou et al., 2021). Oxidation flow reactors (OFRs) enable the simulation of several
86 days of atmospheric aging in a few minutes, with minimized wall effects compared to traditional smog chamber
87 experiments (Palm et al., 2016; Bruns et al., 2015). OFRs have been utilized in numerous studies to investigate the SOA
88 potential of ambient air and emissions from different sources, including motor exhausts (Simonen et al., 2017; Kuittinen et
89 al., 2021; Bruns et al., 2015; Tkacik et al., 2014; Watne et al., 2018; Liu et al., 2019b; Yao et al., 2022; Zhou et al., 2021). For
90 real-world traffic measurement studies using point sampling, OFRs with short response times enable the investigation of a
91 large number of vehicles, thus capturing the large variability between individual vehicles in a fleet (Watne et al., 2018; Zhou
92 et al., 2021; Liao et al., 2021; Ghadimi et al., 2023).

93

94 In this study, we present the findings from the photochemical aging of emissions from a modern on-road bus fleet operating
95 on diesel (DSL) and the latest generation of alternative fuels, including compressed natural gas (CNG), rapeseed methyl ester
96 (RME), and hydrotreated vegetable oil (HVO), using an oxidation flow reactor (Gothenburg Potential Aerosol Mass Reactor,
97 Go:PAM). We aim to compare the secondary production of PM from individual buses in real traffic with their primary PM
98 emissions, examining the impact of fuel type, engine technology, and photochemical age. Furthermore, both fresh and aged
99 emissions of gas and particle phases are characterized using HR-ToF-CIMS, providing a comprehensive understanding of the
100 emissions profile and their environmental implications.

101



102 2. Methods

103 2.1 Emission measurements

104 Roadside measurements were conducted at a designated urban bus stop, featuring a bus-only lane, in Gothenburg, Sweden.
105 (Supporting information (SI), Figure S1). Extractive sampling of individual bus plumes in real traffic was used to characterize
106 emissions, adhering to the method outlined by Hallquist et al. (2013). More details of the experimental conditions are available
107 in our prior publication by Liu et al. (2019a). The primary focus of this study was to utilize the OFR Go:PAM and the HR-
108 ToF-CIMS to explore the potential for secondary pollutant formation and to conduct a detailed chemical characterization of
109 both gas and particle phase compounds. An experimental schematic of the roadside sampling is shown in Figure S2. Briefly,
110 the emissions from passing bus plumes were characterized as they accelerated from standstill at the bus stop. A camera was
111 positioned at the roadside to capture bus plate numbers, facilitating bus identification and enabling the collection of specific
112 information on each bus, including fuel type, engine technology, and exhaust after-treatment systems. The effective
113 identification of emissions from individual buses was achieved by employing CO₂ as a tracer, as delineated by Hak et al.
114 (2009). The concentration of CO₂ was measured with a non-dispersive infrared gas analyzer (LI-840A, time resolution 1 Hz).
115 NO and NO_x were measured with two separate chemiluminescent analyzers (Thermo Scientific™ Model 42i NO-NO₂-NO_x
116 Analyzer). In addition, specific gaseous compounds like CO, NO, and HC, were measured using a remote sensing device
117 (AccuScan RSD 3000, Environmental System Products Inc.). Particle emissions were characterized using a high time
118 resolution engine exhaust particle sizer spectrometer (EEPS, Model 3090 TSI Inc., time resolution 10 Hz) across a size range
119 of 5.6-560 nm. Due to the lack of detailed knowledge about the chemical composition of the emitted particles, particle mass
120 calculations were based on the assumption of spherical particles of unit density.

121
122 The HR-ToF-CIMS coupled with a FIGAERO was used to derive chemical information of both gas and particle phase species.
123 A detailed description of the configuration of the instrument can be found elsewhere (Aljawhary et al., 2013; Lopez-Hilfiker
124 et al., 2014; Le Breton et al., 2018; Le Breton et al., 2019). Acetate, employed as the reagent ion, was generated using an acetic
125 anhydride permeation source through a ²¹⁰Po ion source (²¹⁰Po inline ionizer, NRD inc, Static Solutions Limited). In the ion-
126 molecular reaction (IMR) chamber, the gaseous sampling flow interacted with the reagent ions, leading to the ionization of
127 target molecules. The dual inlets of the FIGAERO enable simultaneous gas phase sampling directly into the IMR and particle
128 sample collection on a PTFE filter for the duration of the plume via a separate inlet. The duration of the target plume for
129 particle collection was indicated by PN concentration measured by the EEPS. Once the PN concentration reduced to
130 undistinguishable at background levels, the filter was automatically positioned to allow the collected particles to be evaporated
131 into the IMR. The nitrogen flow over the filter was incrementally heated from room temperature to 200°C within 5 minutes
132 and then maintained at this maximum temperature for 8 minutes, ensuring complete desorption of mass from the filter, followed
133 by analysis via HR-ToF-CIMS. Perfluoropentanoic acid (PFPA), a reliable high mass calibrant, was injected into the CIMS
134 inlet during the sampling period (Le Breton et al., 2019). Mass spectra were calibrated using known masses (m/z), accurate



135 within 4 ppm: O_2^- , CNO^- , $C_3H_5O_3^-$, $C_2F_3O_3^-$, $C_3F_9O_2^-$, $C_{10}F_{18}O_4^-$, covering a range of 32-526 m/z (more details can be found
136 in SI). The data were acquired at 1 s time resolution. To estimate absolute EFs, a conversion of the CIMS signal to concentration
137 using a sensitivity factor is necessary. Based on the method of Lopez-Hilfiker et al. (2015), the maximum sensitivity was
138 determined to be 20 Hz ppt⁻¹, which falls within previously reported ranges (Mohr et al., 2017). Using this maximum
139 sensitivity provides a lower-limit estimate of EFs for all oxygenated volatile organic compounds (Zhou et al., 2021). The
140 assumption on sensitivity did not affect the comparative analysis of EFs with respect to different fuel types.

141

142 The EFs of constituents per kilogram of fuel burnt were calculated by relating the concentration change of a specific compound
143 in the diluted exhaust plume to the change in CO₂ concentration. CO₂ served as a tracer for exhaust gas dilution, relative to
144 background concentration (Hallquist et al., 2013; Janhäll and Hallquist, 2005; Watne et al., 2018; Hak et al., 2009). In the
145 calculations, complete combustion and carbon contents of 86.1, 77.3, 70.5, and 69.2% for DSL, RME, HVO, and CNG,
146 respectively, were assumed (Edwards et al., 2004). Further methodological details are elaborated in Liu et al. (2019a).

147

148 2.2 Oxidation flow reactor setup

149 The OFR Go:PAM was utilized for photochemical aging of emissions from individual buses to investigate the potential for
150 secondary pollutant formation. The comprehensive description and operational protocols of the Go:PAM have been detailed
151 previously (Watne et al., 2018; Zhou et al., 2021). Briefly, the Go:PAM is a 6.1 L continuous-flow quartz glass flow reactor
152 with input flows such that the median residence time is approximately 37s. The reactor is equipped with two Philips TUV 30
153 W fluorescent lamps ($\lambda = 254$ nm) and enclosed by reflective and polished aluminium mirrors to ensure a homogeneous photon
154 field. The UV lamps generate OH radicals through the photolysis of O₃ in the presence of water vapor. The relative humidity
155 (RH) within the reactor was around 60 - 80%. The O₃ concentration inside the Go:PAM was measured using an ozone monitor
156 (2B technology, model 205 dual beam ozone monitor) at around 880 ppb prior to the introduction of vehicle exhaust. Particle
157 wall losses in the Go:PAM were corrected using size-dependent transmission efficiency (Watne et al., 2018). The OH exposure
158 (OH_{exp}) inside the Go:PAM was calibrated offline using sulfur dioxide (SO₂), following methodologies established in previous
159 studies (Lambe et al., 2011; Kang et al., 2007), with additional details provided in the SI. During on-road measurements, the
160 OH_{exp} may be significantly influenced by the OH reactivity (i.e., CO and HC) and titration of O₃ by NO in the plumes, which
161 varied between vehicles. Thus, the OH reactivity was estimated for each bus passage using the maximum NO_x, CO and HC
162 concentrations in the Go:PAM, along with corresponding water and ozone levels (Watne et al., 2018; Zhou et al., 2021).
163 Employing the maximum concentrations of these OH- or O₃-consuming species represents a minimum estimate of OH_{exp} in
164 our calculations. The flow-design incorporated in the Go:PAM enables investigation of transient phenomena, such as passing
165 plumes. It also works at relatively low ozone concentrations (less than 1 ppm), limiting reactions of other potential oxidants
166 such as O₃, NO₃, or O¹D (Zhou et al., 2021).

167

168



169 3. Results and discussion

170 3.1 Fresh and aged PM emissions from buses

171 The aged PM emissions ($EF_{PM:aged}$) of 133 plumes from a diverse set of buses, including 16 DSL, 11 CNG, 20 RME, 20 HVO
172 and 9 hybrid-electric HVO (HVO_{HEV}) buses, were investigated using Go:PAM. The corresponding average fresh PM emissions
173 ($EF_{PM:Fresh}$) for these 76 buses were measured during several sequential days (Figure S2). These buses were a subset of the 234
174 buses described in our previous study (Liu et al., 2019a), and represent data corresponding to available Go:PAM
175 measurements. A comprehensive discussion on the full data set for fresh condition is available in Liu et al. (2019a). Figure 1
176 shows the average $EF_{PM:Fresh}$ and $EF_{PM:aged}$ with respect to fuel type. Among the buses, Euro V DSL models had the highest
177 median $EF_{PM:Fresh}$, $MdEF_{PM:Fresh}$ (represented by the horizontal yellow lines), of 208 mg kg-fuel⁻¹, followed by HVO_{HEV} , RME
178 and HVO buses with $MdEF_{PM:Fresh}$ of 109, 74 and 62 mg kg-fuel⁻¹ respectively. CNG buses and HVO_{HEV} buses equipped with a
179 DPF under Euro VI standards exhibited the lowest $MdEF_{PM:Fresh}$, with over half of these buses exhibiting $EF_{PM:Fresh}$ below the
180 detection limit (<4.3 mg kg-fuel⁻¹). Except for HVO_{HEV} buses with a DPF, which was limited to a small tested number, all
181 other bus types in this subset had $MdEF_{PM:Fresh}$ comparable to those of the full data set in Liu et al. (2019a), within $\pm 30\%$ and
182 following the same rank order. The average EFs of fresh and aged particle emissions and general gaseous pollutants for
183 individual buses are given in Table 1.

184

185 After photooxidation in Go:PAM, particle mass increased markedly, with half of the individual buses showing average
186 $EF_{PM:aged}$ more than eight times their average $EF_{PM:Fresh}$. For all Euro V/EEV buses, the median $EF_{PM:aged}$, $MdEF_{PM:aged}$
187 (represented by the horizontal blue lines), was highest for DSL buses of 749 mg kg-fuel⁻¹ followed by a descending order of
188 RME (655) > CNG (645) > HVO (543) > HVO_{HEV} (509). Despite low $EF_{PM:Fresh}$, CNG buses produced substantial secondary
189 particle mass. The DPF, proven effective in earlier studies (Martinet et al., 2017; Preble et al., 2015; May et al., 2014),
190 efficiently reduced primary particle emissions from DSL Euro III and HVO_{HEV} Euro VI buses. However, these bus types, even
191 with DPFs, exhibited higher $EF_{PM:aged}$ than those using the same fuels but without DPFs (Euro V), albeit the number of tested
192 buses with DPFs was limited. The variance in median $EF_{PM:aged}$ among different fuel types was less pronounced compared to
193 $EF_{PM:Fresh}$, suggesting the presence of significant non-fuel-dependent precursor sources (Watne et al., 2018; Le Breton et al.,
194 2019).

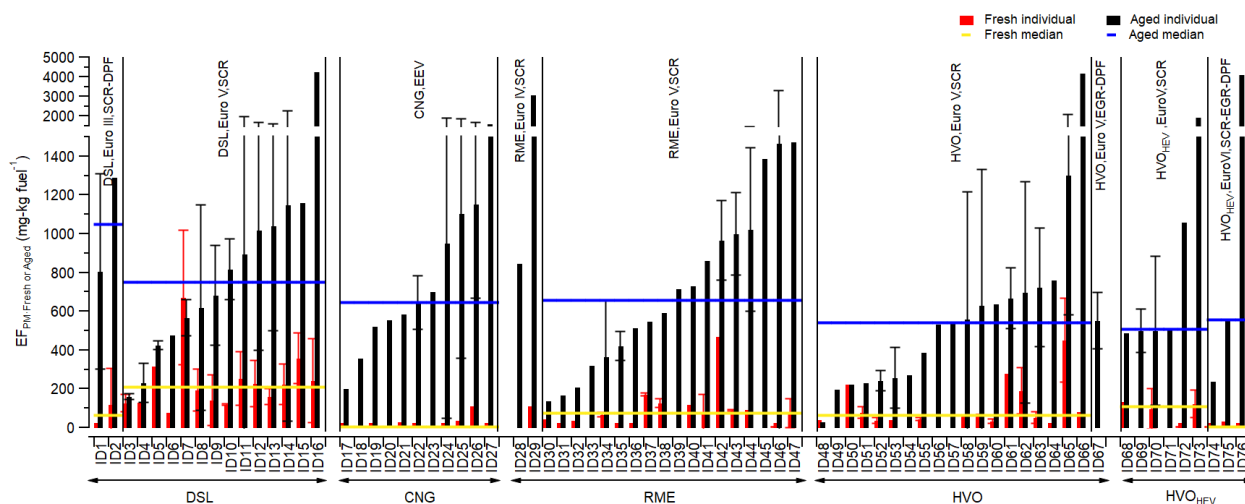
195

196 Figure 2 shows the bus average $EF_{PM:Fresh}$ vs the corresponding $EF_{PM:aged}$ for individual bus passages, where the average
197 $EF_{PM:aged}$ for each bus is indicated by a solid horizontal line. This analysis focuses on Euro V/EEV buses to ensure high number
198 of buses in the comparison, while buses from other Euro classes were not included due to their limited numbers. $EF_{PM:aged}$
199 exhibited notable variation between passages of the same bus, likely attributable to emission variability between passages and
200 differing dilution levels for plumes prior to sampling into the Go:PAM. The median ratio of $EF_{PM:aged}$ to $EF_{PM:Fresh}$ was highest
201 for CNG buses (84), followed by RME (10.8), HVO_{HEV} (10.5), HVO (6.7) and DSL(4.0) buses. Buses equipped with DPFs,



202 including DSL Euro III and HVO_{HEV} Euro VI (not included in Figure 2), exhibited a median ratio exceeding 50. In Figure 2b,
 203 $EF_{PM:Fresh}$ and $EF_{PM:aged}$ are presented as a function of the dilution level, indicated by the integrated CO₂ area. Some buses had
 204 primary emissions too dilute for detection (markers located to the left in Figure 2b) but still showed non-negligible $EF_{PM:aged}$
 205 upon oxidation. To examine the effects of simulated atmospheric oxidation in the Go:PAM, an estimated minimum OH_{exp} was
 206 calculated for each plume by incorporating the OH reactivities of CO and HC and the titration of O₃ with NO, following
 207 methodologies from Watne et al. (2018) and Zhou et al. (2021). For all plumes, OH_{exp} varied between 1.1×10^9 to 4.6×10^{11}
 208 molecules cm⁻³ s. The $EF_{PM:aged}$ for some buses, for example, the DSL and HVO located to the right in Figure 2c, increased
 209 with increasing OH_{exp} . However, due to potential large differences in emissions together with dilution effects across different
 210 passages, the OH_{exp} dependent $EF_{PM:aged}$ for other buses was less pronounced.

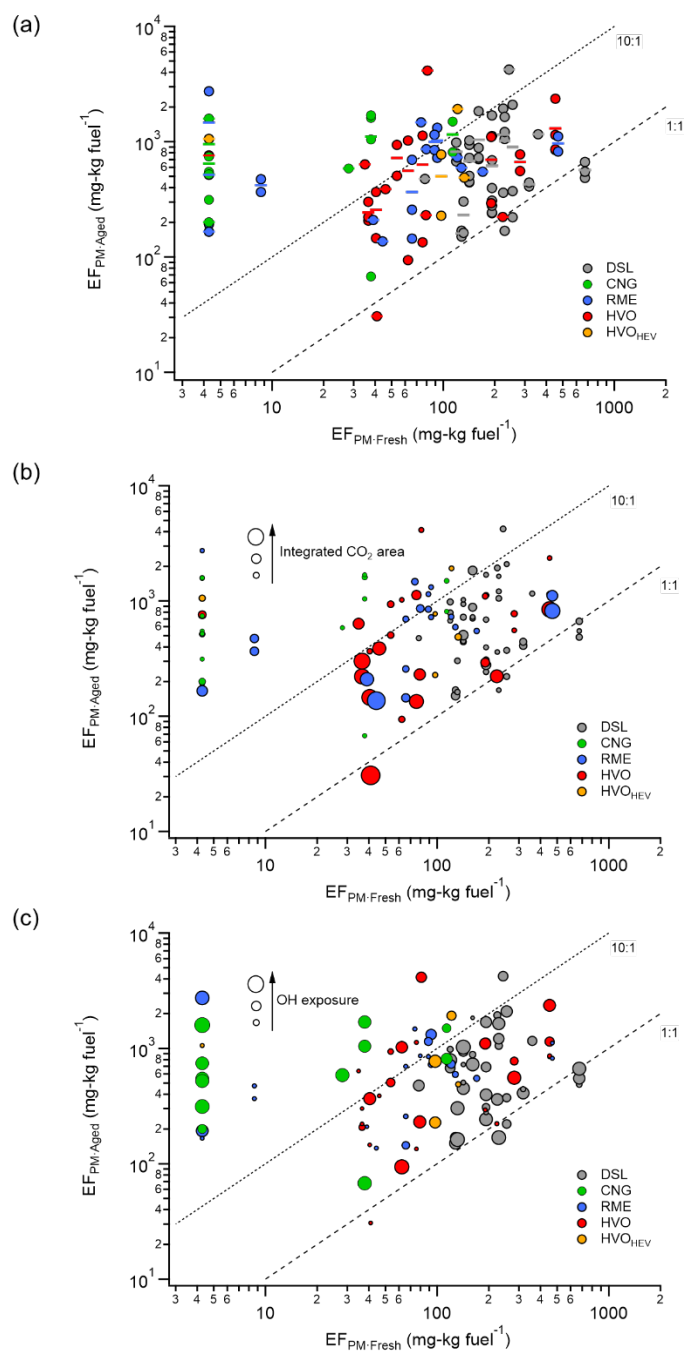
211



212

213 Figure 1. $EF_{PM:Fresh}$ (red bar) and $EF_{PM:aged}$ (black bar) with respect to fuel class: DSL (diesel, ID₁-ID₁₆), CNG (compressed
 214 natural gas, ID₁₇-ID₂₇), RME (rapeseed methyl ester, ID₂₈-ID₄₇), HVO (rapeseed methyl ester, ID₄₈-ID₆₇) and HVO_{HEV} (hybrid-
 215 electric HVO, ID₆₈-ID₇₆) buses. The information on engine technology and exhaust after-treatment systems is also shown.
 216 Given errors represent the standard deviation (1σ).

217



218

219

220 Figure 2. $EF_{PM:aged}$ vs average $EF_{PM:Fresh}$ for all the studied bus passages (Euro V) with respect to fuel type (a) and as a function
221 of integrated CO₂ area (b) and OH exposure (OH_{exp}) (c). The dashed lines denote the 10:1 and 1:1 $EF_{PM:aged}$: $EF_{PM:Fresh}$ ratios,



222 and the solid lines in (a) represent bus averages. One may note that the buses with $EF_{PM:Fresh}$ values below detection limit were
 223 set to $4.3 \text{ mg kg-fuel}^{-1}$.

224

225 Table 1. Average particle and gaseous EFs of individual buses for fresh emissions and average EF_{PM} for aged emissions^a.

Bus ID	Fuel ^c	Euro standard	Exhaust after-treatment system ^d	$EF_{PM:Fresh}$ (mg kg^{-1}_{fuel})	$EF_{PN:Fresh}$ ($10^{14}\# \text{ kg}^{-1}_{fuel}$)	EF_{CO} (g kg^{-1}_{fuel})	EF_{THC} (g kg^{-1}_{fuel})	EF_{NOx} (g kg^{-1}_{fuel})	$EF_{PM:Aged}$ (mg kg^{-1}_{fuel})
1	DSL	III	SCR, DPF	4.3	0.41	3.9±11	1.5±2.9	10±3.2	810±510
2	DSL	III	SCR, DPF	120±190	34±61	2.7±7	1.7±3.7	11±5	1300
3	DSL	V	SCR	130±45	3.3±1.3	17±18	0.35±1.3	3.9±3.7	160±13
4	DSL	V	SCR	130	3.6	20±22	1.5±3.6	4.7±7.2	230±100
5	DSL	V	SCR	320	5.9	20±28	2±3.5	9.7±7	430±23
6	DSL	V	SCR	78	1.6	20±21	2.7±5.6	13±12	480
7	DSL	V	SCR	670±350	10±6.8	42±44	2.3±3.7	6.8±5	570±92
8	DSL	V	SCR	190±110	6.5±3	14±21	0.75±1.7	12±5.1	620±530
9	DSL	V	SCR	140±130	4.3±2.6	9.8±14	1±1.5	15±13	680±260
10	DSL	V	SCR	120±4.7	3.2±0.66	16±18	2.5±4.7	12±6.9	820±160
11	DSL	V	SCR	250±140	4.7±2.7	16±23	0.8±1.4	12±8.9	900±1000
12	DSL	V	SCR	230±120	5.1±1.5	16±26	2.6±4.6	12±9.9	1000±620
13	DSL	V	SCR	160±41	3.5±0.97	27±27	1.4±2.7	17±9.8	1000±540
14	DSL	V	SCR	220±110	5.2±1.3	12±17	2.6±4.1	11±7.4	1100±1100
15	DSL	V	SCR	360±130	6.8±4.2	21±25	1.2±3.3	5.7±4.4	1200
16	DSL	V	SCR	240±220	22±11	5.5±7.5	0.74±1.6	6.8±5.6	4200
17	CNG	EEV	-	4.3±0	0.41±0	n.a.	n.a.	4.8±1.7	200
18	CNG	EEV	-	n.a.	n.a.	n.a.	n.a.	11±4.9	360
19	CNG	EEV	-	4.3±0	0.41±0	n.a.	n.a.	4±3.8	520
20	CNG	EEV	-	n.a.	n.a.	n.a.	n.a.	15±17	560
21	CNG	EEV	-	28	1.3	n.a.	n.a.	2.2±0.93	590
22	CNG	EEV	-	4.3	0.41	n.a.	n.a.	1.8±1	650±140
23	CNG	EEV	-	n.a.	n.a.	n.a.	n.a.	3.2±0.53	700
24	CNG	EEV	-	4.3	0.41	n.a.	n.a.	6.9±1.4	950±900
25	CNG	EEV	-	38	11	n.a.	n.a.	7.3±5.3	1100±750
26	CNG	EEV	-	110	200	n.a.	n.a.	8.2±4.2	1200±480
27	CNG	EEV	-	4.3±0	0.41±0	n.a.	n.a.	6±1.8	1600
28	RME	IV	SCR	n.a.	n.a.	10±8.7	3.1±3	46±20	850
29	RME	IV	SCR	110	4.1	4.2±8.4	0.19±0.38	7.2±6.8	3000
30	RME	V	SCR	44	2.2	12±14	2.2±3.6	32±32	140
31	RME	V	SCR	4.3	0.41	7.4±7.1	0.075±0.17	13±5.1	170
32	RME	V	SCR	39	6.2	5.2±4.8	0.87±1.1	18±5.4	210
33	RME	V	SCR	n.a.	n.a.	0.24±0.54	0.24±0.39	10±3.3	320
34	RME	V	SCR	66±11	2.4±1	7±7.2	1.8±2.7	23±13	370±290
35	RME	V	SCR	8.6	0.96	4.9±3.6	0.59±0.73	20±5.1	420±75
36	RME	V	SCR	4.3	0.41	22±23	1.8±2	25±16	520
37	RME	V	SCR	170±7.7	6.4±1	34±35	0.016±0.043	19±10	550
38	RME	V	SCR	130±24	11±14	17±20	2±4	16±15	590
39	RME	V	SCR	n.a.	n.a.	1.2	0.64	21	720
40	RME	V	SCR	120	5.3	12±9.4	1.8±2.6	18±8.2	730
41	RME	V	SCR	80±95	4.2±2.9	8.8±17	0.72±0.87	25±5.7	860
42	RME	V	SCR	470	5.8	4.5±5.1	0.23±0.38	18±7.8	970±210
43	RME	V	SCR	89±2.3	2.6±0.16	5.4±9.4	0.68±1.9	28±17	1000±210
44	RME	V	SCR	92	1.6	14±19	1.8±3	23±17	1000±420
45	RME	V	SCR	n.a.	n.a.	37±26	5.8±3.6	14±6.3	1400
46	RME	V	SCR	4.3±0	0.41±0	9.6±14	0.89±1.4	28±8.4	1500±1800
47	RME	V	SCR	74±75	12±6	6.1±6.3	1.1±1.4	18±5.2	1500
48	HVO	V	SCR	41	1.5	8.4±2	0.14±0.31	10±0.4	31
49	HVO	V	SCR	n.a.	n.a.	5.8±8	0.7±0.62	13±10	200
50	HVO	V	SCR	220	6.6	8.3±9.1	0.91±0.97	13±8.6	220
51	HVO	V	SCR	79±31	2.6±0.74	7.8±5.8	0.41±0.59	12±8.2	230



52	HVO	V	SCR	37±13	1.9±0.65	4.8±5.5	0.64±0.82	20±3	240±51
53	HVO	V	SCR	40	2.5	2.1±3.4	0.0083±0.019	16±4.3	260±160
54	HVO	V	SCR	n.a.	n.a.	2.1±3	0.55±0.77	22	270
55	HVO	V	SCR	46±6.6	2.6±0.52	6.2±4.1	0.79±0.55	12±8.2	390
56	HVO	V	SCR	n.a.	n.a.	11±10	0.74±0.84	5.7	530
57	HVO	V	SCR	n.a.	n.a.	14±17	0.79±1.2	11±2.6	540
58	HVO	V	SCR	62	4.1	6.8±6.7	0.22±0.31	11±6.3	560±660
59	HVO	V	SCR	76	5.3	2.3±2	0.24±0.47	19±3.4	630±700
60	HVO	V	SCR	35±11	1.5±0.19	3.3±5	0.45±0.86	9.2±9	640
61	HVO	V	SCR	280	14	9.9±16	0.55±0.73	11±3.6	670±160
62	HVO	V	SCR	190±120	68±86	1.1±1.9	0.3±0.49	9.3±4.9	700±570
63	HVO	V	SCR	54±30	4.6±2.2	3.5±4.6	0.49±0.48	14±3.5	720±310
64	HVO	V	SCR	4.3	0.41	2.2±3.8	0.33±0.73	12±4.8	760
65	HVO	V	SCR	450±220	18±18	1.4±1.6	0.28±0.37	12±2.6	1300±720
66	HVO	V	SCR	81	11	0.88±0.93	0.28±0.25	13±6.5	4100
67	HVO	V	EGR, DPF	n.a.	n.a.	4.6±5.9	0.64±1.2	11±8.1	550±150
68	HVO _{HEV}	V	SCR	130	52	12±19	0.97±1.4	20±15	490
69	HVO _{HEV}	V	SCR	n.a.	n.a.	4.1±8.4	0.5±1.3	18±3.3	500±110
70	HVO _{HEV}	V	SCR	97±100	25±18	3.8±6.8	1.1±1.8	17±5.7	500±390
71	HVO _{HEV}	V	SCR	n.a.	n.a.	7.6±9.9	2.9±2.4	12±2.1	520
72	HVO _{HEV}	V	SCR	4.3±0	0.41±0	3.7±5.8	1±2.4	20±10	1100
73	HVO _{HEV}	V	SCR	120±72	8.9±2.9	1.2±1.7	0.18±0.26	17±7	1900
74	HVO _{HEV}	VI	SCR,EGR,DPF	4.3±0	0.41±0	4.7±11	2.2±4.7	7.2±8.5	240
75	HVO _{HEV}	VI	SCR,EGR,DPF	33	29	1.2±2.4	0.22±0.49	6.7±3.3	550
76	HVO _{HEV}	VI	SCR,EGR,DPF	4.3	0.41	10±9.2	1.5±2.3	8.8±8.7	4100

226

227

^aGiven errors represent the standard deviation (1σ).

228

^bn.a., abbreviation for not available.

229

^cDSL, CNG, RME, HVO and HVO_{HEV}, abbreviations for diesel, compressed natural gas, rapeseed methyl ester, hydrotreated vegetable oil, and hybrid-electric hydrotreated vegetable oil.

230

^dSCR, DPF and EGR, abbreviations for selective catalytic reduction, diesel particulate filter and exhaust gas recirculation systems.

231

232

233

234

235 The secondary particle mass formed (ΔPM) was calculated as the difference between $EF_{PM:aged}$ for a plume and the average
 236 $EF_{PM:Fresh}$ for the corresponding individual bus. Figure 3 shows the ΔPM as a function of OH_{exp} for all bus types during the
 237 Go:PAM measurements. The results in this study are compared with those reported from a tunnel study (Tkacik et al., 2014),
 238 an urban roadside study of a mixed fleet in Hong Kong (Liu et al., 2019b), a depot study on rather modern types of city
 239 buses (Watne et al., 2018) and roadside measurements of a heavy-duty truck fleet in Gothenburg (Zhou et al., 2021).
 240 Laboratory OFR and chamber studies of middle-duty and heavy-duty diesel vehicles (Deng et al., 2017), diesel passenger
 241 cars (Chirico et al., 2010), a diesel engine (Jathar et al., 2017a), and gasoline vehicles (Gordon et al., 2014a; Platt et al.,
 242 2013) were also included for comparison.

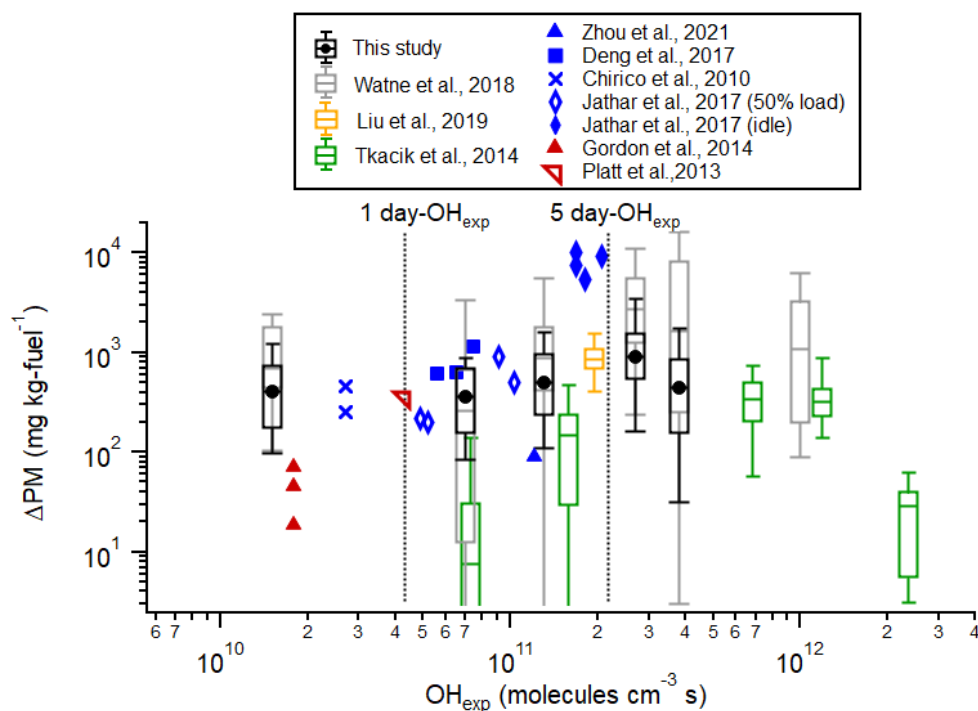
243

244 The ΔPM from vehicle emissions is influenced by factors such as vehicle and fuel types, driving modes, and OH_{exp} during
 245 experiments (Gentner et al., 2017). Considering the variability of OH reactivity among vehicles and the consequently wide
 246 range of OH_{exp} , this study, along with Watne et al. (2018), categorizes ΔPM trend into OH_{exp} bins. The median ΔPM was
 247 approximately $400 \text{ mg kg-fuel}^{-1}$ at $OH_{exp} < 4.3 \times 10^{10} \text{ molecules cm}^{-3} \text{ s}$ (corresponding to 1 OH day, assuming an OH
 248 concentration of $1 \times 10^6 \text{ molecules cm}^{-3}$ for 12 h per day) and was $364\text{--}495 \text{ mg kg-fuel}^{-1}$ at 1-5 OH days, reaching a maximum
 249 of around $920 \text{ mg kg-fuel}^{-1}$ at approximately 5-6 OH days for the bus fleet in this study, comprising 40% DSL, 12.2% CNG,



250 20% RME, 20.8% HVO, and 7% HVO_{HEV} buses. This peak value of ΔPM was lower than the approximately 3000 mg kg-fuel⁻¹
 251 ¹ at ~5-6 OH days observed in the depot measurements by Watne et al. (2018), a difference potentially due to variations in
 252 engine technology and fuel types used in the bus fleets. Notably, HVO was not used in the depot study, while some buses
 253 switched from RME to HVO prior to this study. The ΔPM peaked and then decreased at higher OH_{exp}, likely due to the
 254 transition from functionalization-dominated reactions and condensation at lower OH_{exp} to fragmentation reactions and
 255 evaporation dominance at higher OH_{exp} (Tkacik et al., 2014; Ortega et al., 2016). The ΔPM in this study was comparable to
 256 855 mg kg-fuel⁻¹ for a mixed fleet consisting of 44.1% gasoline, 41.3% diesel, and 14.6% LPG vehicles measured at an urban
 257 roadside in Hong Kong (Liu et al., 2019b), and was slightly higher than that of a Euro VI dominated (more than 70%) heavy-
 258 duty truck fleet measured at an urban roadside site in Gothenburg (Zhou et al., 2021). Additionally, the ΔPM in this study was
 259 consistent with that for middle-duty and heavy-duty diesel vehicles (Deng et al., 2017), diesel passenger cars (Chirico et al.,
 260 2010), and a diesel (or biodiesel)-fuelled engine under 50% load condition (Jathar et al., 2017a) (around 190-1133 mg kg-
 261 fuel⁻¹). However, the diesel (or biodiesel)-fuelled engine under idle conditions can produce significantly higher ΔPM (more
 262 than 5000 mg kg-fuel⁻¹), likely because engines at idle loads are less efficient at burning fuel, leading to higher emissions of
 263 unburnt gaseous combustion products (as precursors of secondary PM) (Nordin et al., 2013; Saliba et al., 2017; Jathar et al.,
 264 2017a). In contrast, experiments conducted for gasoline vehicles at relatively low photochemical ages (< 1 OH day) typically
 265 produced ΔPM lower than 70 mg kg-fuel⁻¹ (Gordon et al., 2014a), except for a Euro 5 gasoline vehicle (340 mg kg-fuel⁻¹)
 266 operated with a New European Driving Cycle (Platt et al., 2013).

267



268



269

270 Figure 3. Secondary particle mass formed (ΔPM), calculated as $\text{EF}_{\text{PM:aged}}$ subtracted by the average $\text{EF}_{\text{PM:Fresh}}$, vs modeled OH
271 exposure (OH_{exp}) for the bus fleet in this study and comparison with those reported for a tunnel study (Tkacik et al., 2014), a
272 depot study (Watne et al., 2018), roadside measurements (Liu et al., 2019b; Zhou et al., 2021), middle-duty and heavy-duty
273 diesel vehicles (Deng et al., 2017), diesel passenger cars (Chirico et al., 2010), a diesel engine (Jathar et al., 2017a), and
274 gasoline vehicles (Gordon et al., 2014a; Platt et al., 2013). Dashed lines indicate 1- and 5-day OH_{exp} assuming an OH
275 concentration of 1×10^6 molecules cm^{-3} 12 h per day (Watne et al., 2018). Note that ΔPM in this study, alongside those by
276 Watne et al. (2018), Zhou et al. (2021) and Liu et al. (2019b), includes both secondary organic and inorganic aerosol, while
277 ΔPM in research by Deng et al. (2017), Chirico et al. (2010), Jathar et al. (2017a), Gordon et al. (2014a), Platt et al. (2013)
278 and Tkacik et al. (2014) pertains only to secondary organic aerosol mass.

279

280

281

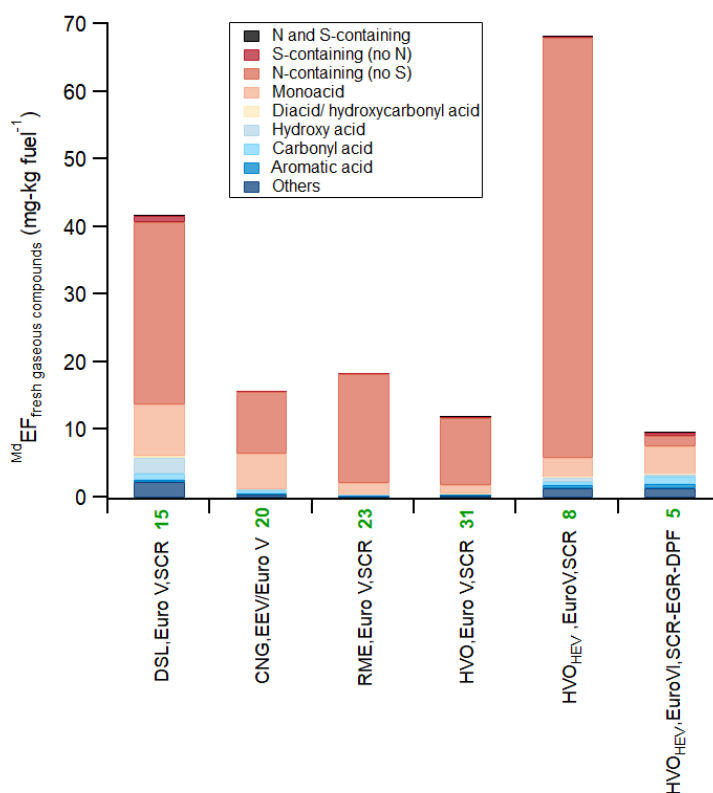
282 3.2 Chemical characterization using CIMS

283 3.2.1 Fresh gaseous emissions

284 Figure 4 presents the median emission factors ($^{\text{M}}\text{dEFs}$) of CIMS measured fresh gaseous emissions with respect to fuel type.
285 The identities of the organic compounds detected by HR-ToF-CIMS are assigned based on knowledge of sensitivities of the
286 ionization scheme and the expected compounds emitted from the buses. Plausible compounds are assigned from the formulae,
287 with a caveat that other isomers might contribute to the signal. These compounds were classified into nine families based on
288 their molecular characteristics as outlined by Liu et al. (2017), with additional details provided in the SI. Among all Euro
289 V/EEV buses, hybrid-electric HVO (HVO_{HEV}) buses exhibited the highest $^{\text{M}}\text{dEF}$ of CIMS measured fresh gaseous emissions
290 ($68 \text{ mg kg-fuel}^{-1}$), followed by DSL ($42 \text{ mg kg-fuel}^{-1}$), RME ($18 \text{ mg kg-fuel}^{-1}$), and CNG ($16 \text{ mg kg-fuel}^{-1}$), while HVO had
291 the lowest $^{\text{M}}\text{dEF}$ of $12 \text{ mg kg-fuel}^{-1}$. Nitrogen (N)-containing compounds (no sulfur) and monoacid families predominantly
292 composed these fresh gaseous emissions. Compared to Euro V HVO_{HEV} buses, HVO_{HEV} buses equipped with exhaust gas
293 recirculation (EGR) and DPF systems (Euro VI) demonstrated a significant reduction in $^{\text{M}}\text{dEF}$ ($10 \text{ mg kg-fuel}^{-1}$), primarily due
294 to decreased emissions of N-containing compounds, although the $^{\text{M}}\text{dEF}$ of other compound families were higher. In contrast,
295 Zhou et al. (2021) reported significant reductions in both carboxylic acids and carbonyl compounds (by 94% on average), and
296 acidic nitrogen-containing organic and inorganic species (79%) when transitioning from Euro V to Euro VI heavy-duty trucks.
297 However, details on the types of exhaust after-treatment systems used in the trucks from such study are not specified.
298 Moreover, this study utilized acetate as a different reagent ion for CIMS compared to the iodide used by Zhou et al. (2021).
299 Table 2 lists the top 10 $^{\text{M}}\text{dEFs}$ of fresh gaseous compounds, contributing over 88% of total fresh gaseous emissions measured
300 by CIMS for most bus types, except for Euro VI HVO_{HEV} (61%). The fresh gaseous emissions from all types of Euro V/EEV
301 buses were primarily composed of nitrous acid (HONO) and nitric acid (HNO_3), with HONO being the most significant acidic
302 emission. The $^{\text{M}}\text{dEFs}$ of HONO and HNO_3 generally align with values reported in the literature, ranging from approximately



303 7-250 mg kg-fuel⁻¹ for HONO (Nakashima and Kondo, 2022; Kurtenbach et al., 2001; Liao et al., 2020; Wentzell et al., 2013)
 304 and around 4-14 mg kg-fuel⁻¹ for HNO₃ (Wentzell et al., 2013). Acetic acid (C₂H₄O₂), formic acid (CH₂O₂), and isocyanic acid
 305 (HNCO) also exhibited relatively high ^{Md}EFs. The ^{Md}EFs of formic acid for all Euro V/EEV bus types (0.02-1.97 mg kg-fuel⁻¹)
 306 ¹) were consistent with those from a light-duty gasoline fleet (0.57–0.94 mg kg-fuel⁻¹) reported by Crisp et al. (2014). The
 307 ^{Md}EFs of acetic acid ranged from 1.23 to 4.84 mg kg-fuel⁻¹, falling between values for gasoline vehicles (0.78 mg kg-fuel⁻¹)
 308 and diesel buses (approximately 12-23 mg kg-fuel⁻¹) (Li et al., 2021). Isocyanic acid, likely an intermediate product of thermal
 309 degradation of urea in SCR systems without sufficient hydrolysis (Bernhard et al., 2012), was detected in emissions from all
 310 bus types, with ^{Md}EFs of 0.08-14.74 mg kg-fuel⁻¹. These values are slightly lower than those from a non-road diesel engine
 311 (31-56 mg kg-fuel⁻¹) reported by Jathar et al. (2017b), but align well with SCR-equipped diesel vehicles tested by Suarez-
 312 Bertoa and Astorga (2016) (1.3-9.7 mg kg-fuel⁻¹) and a diesel engine with a diesel oxidation catalyst (DOC) (Wentzell et al.,
 313 2013) (0.21-3.96 mg kg-fuel⁻¹). Among all Euro V/EEV buses, HVO_{HEV} buses showed the highest emissions of HNCO,
 314 potentially attributed to cold engine conditions since the combustion engine does not operate continuously. Notably, emissions
 315 of HNCO were significantly lowered and neither HONO nor HNO₃ were identified among the top 10 ^{Md}EFs for HVO_{HEV} buses
 316 equipped with EGR and DPF systems (Euro VI), suggesting that newer engine technologies incorporating EGR and DPF
 317 systems likely effective in reducing emissions of NO_x (Table 1) as well as HNCO, HONO and HNO₃.
 318





320 Figure 4. ^{Md}EFs of CIMS measured fresh gaseous emissions with respect to fuel class: DSL (diesel, 15), CNG (compressed
321 natural gas, 20), RME (rapeseed methyl ester, 23), HVO (rapeseed methyl ester, 31) and HVO_{HEV} (hybrid-electric HVO, 13)
322 buses. The number in bold green represents the number of buses examined.

323

324

325 Table 2. Summary of top 10 ^{Md}EFs of fresh gaseous compounds measured using HR-ToF-CIMS of DSL, CNG, RME, HVO
326 and HVO_{HEV} buses (color coded by different families shown in Figure 4).

DSL, Euro V, SCR		CNG, EEV/Euro V		RME, Euro V, SCR		HVO, Euro V, SCR		HVO _{HEV} , Euro V, SCR		HVO _{HEV} , Euro VI	
Species	^{Md} EF (mg kg _{fuel} ⁻¹)	Species	^{Md} EF (mg kg _{fuel} ⁻¹)	Species	^{Md} EF (mg kg _{fuel} ⁻¹)	Species	^{Md} EF (mg kg _{fuel} ⁻¹)	Species	^{Md} EF (mg kg _{fuel} ⁻¹)	Species	^{Md} EF (mg kg _{fuel} ⁻¹)
HONO	20.64	HONO	4.92	HONO	12.72	HONO	7.62	HONO	38.96	C ₃ H ₂ O ₂	2.42
HNO ₃	5.29	C ₂ H ₄ O ₂	4.68	HNO ₃	3.24	HNO ₃	2.20	HNCO	14.74	C ₂ H ₄ O ₂	1.23
C ₂ H ₄ O ₂	4.84	HNO ₃	3.48	C ₂ H ₄ O ₂	1.23	C ₂ H ₄ O ₂	1.23	HNO ₃	7.89	C ₂ H ₂ O ₃	0.62
CH ₂ O ₂	1.97	HNCO	0.51	CH ₂ O ₂	0.48	C ₃ H ₆ O ₃	0.14	C ₂ H ₄ O ₂	1.83	C ₈ H ₆ O ₄	0.40
C ₃ H ₆ O ₃	1.79	CH ₂ O ₂	0.30	HNCO	0.15	C ₃ H ₂ O ₂	0.09	CH ₂ O ₂	0.45	C ₆ H ₅ NO ₂	0.31
CH ₄ SO ₃	0.71	C ₂ H ₂ O ₃	0.25	C ₂ H ₂ O ₃	0.05	HNCO	0.08	C ₃ H ₆ O ₃	0.43	HNCO	0.27
HNCO	0.67	C ₃ H ₂ O ₂	0.14	C ₃ H ₈ O ₃	0.03	CH ₂ O ₂	0.02	C ₃ H ₂ O ₂	0.34	C ₃ H ₄ O ₅	0.22
C ₃ H ₄ O ₅	0.37	C ₃ H ₄ O ₂	0.06	CH ₄ SO ₃	0.02	C ₂ H ₂ O ₃	0.02	C ₉ H ₁₀ O ₃	0.16	C ₇ H ₆ O ₃	0.20
C ₂ H ₂ O ₃	0.31	C ₇ H ₆ O ₃	0.05	C ₃ H ₄ O ₂	0.02	C ₃ H ₄ O ₃	0.02	C ₈ H ₆ O ₄	0.12	C ₅ H ₈ O ₃	0.17
C ₄ H ₆ O ₄	0.22	C ₃ H ₈ O ₄	0.05	C ₆ H ₆ N ₂ O ₂	0.01	C ₄ H ₆ O ₄	0.01	C ₃ H ₈ O ₃	0.10	H ₄ N ₂ O ₂ S	0.16

327

328

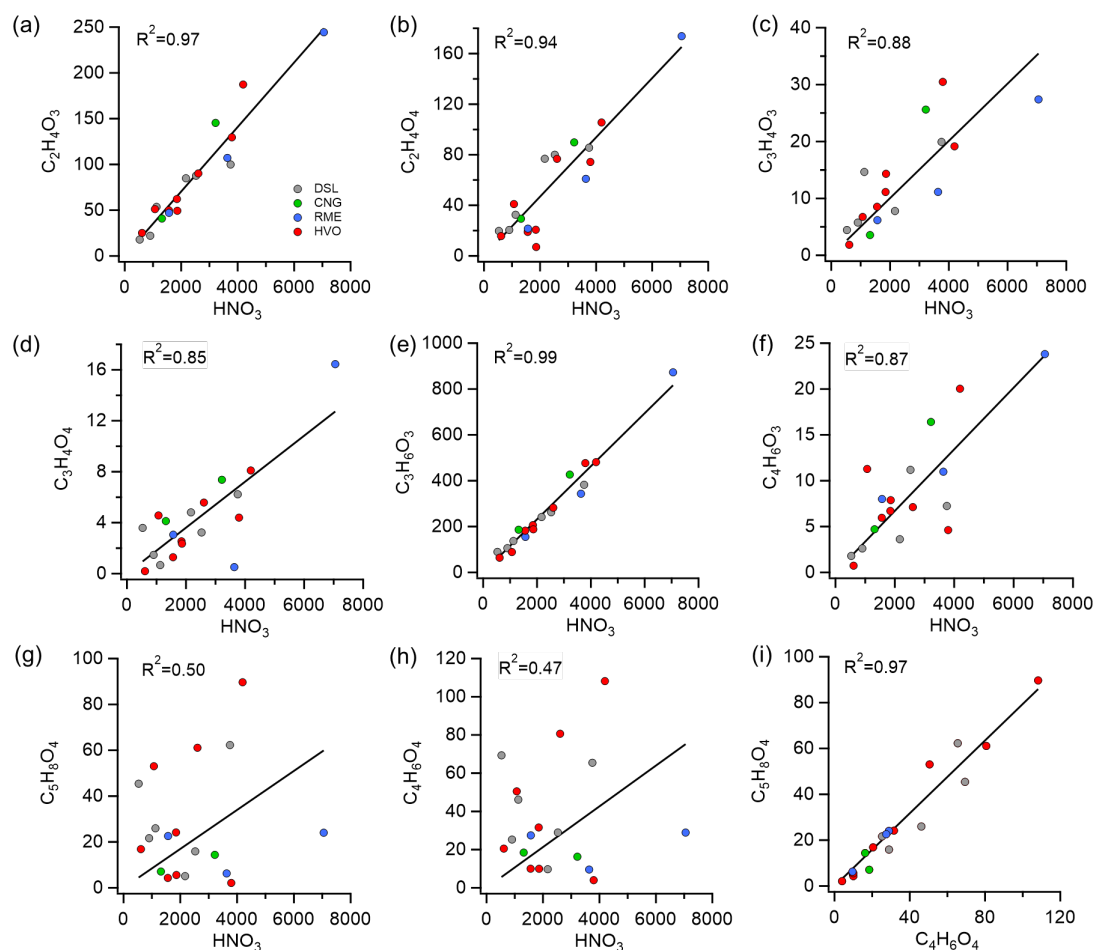
329

330 3.2.2 Aged gaseous emissions

331 Secondary carboxylic acids were measured following exposure of the exhaust to OH. Figure 5 shows the correlations between
332 ion counts of the most abundant gas-phase organic acids and nitric acid (HNO₃) after oxidation in the Go:PAM. HNO₃ serves
333 as an indicator of NO_x oxidation. Most acids exhibited both primary and secondary sources, except for dihydroxyacetic acid
334 (C₂H₄O₄), which was only identified post-aging. The chemical characterization of the aged emissions was conducted on
335 separate occasions using HR-ToF-CIMS, capturing a limited number of buses (N=19). When these buses were categorized by
336 fuel type, the sample size for each category became smaller, constraining statistical comparison across different bus types.
337 Nevertheless, we analyzed the relationship between various chemical species across all buses. Glycolic acid (C₂H₄O₃),
338 dihydroxyacetic acid (C₂H₄O₄), pyruvic acid (C₃H₄O₃), malonic acid (C₃H₄O₄), lactic acid (C₃H₆O₃) and acetoacetic acid
339 (C₄H₆O₃) closely followed the signals of HNO₃ with high correlations (R²= 0.85-0.99, Fig. 5a-f). However, correlations
340 between glutaric acid (C₅H₈O₄) and HNO₃, and between succinic acid (C₄H₆O₄) and HNO₃, were poorer, suggesting different
341 formation mechanisms for these two organic acids compared to the others mentioned. Notably, these two acids showed a strong
342 correlation with each other (R²= 0.97, Fig. 5i) and both belong to the diacid/hydroxycarbonyl acid families. While most of



343 these small organic acids correlated well with HNO_3 , their correlations with $\text{EF}_{\text{PM:aged}}$ or ΔPM were moderate to weak ($R^2 <$
 344 0.6, Figure S4). This possibly indicates that the OH-driven formation of these carboxylic acids occurs on a different time scale
 345 compared to the production of organic aerosol (Friedman et al., 2017), at least in this Go:PAM experiment. This could also be
 346 due to different subsets of hydrocarbon precursors driving the production of organic acids and secondary particle mass.
 347 Similarly, Friedman et al. (2017) observed a lack of correlation between organic aerosol and gaseous organic acid
 348 concentrations downstream of the flow reactor from a diesel engine, indicating that organic acids may not be reliable tracers
 349 for secondary organic aerosol formation from diesel exhaust.
 350



351
 352 Figure 5. Correlations between ion counts of most abundant gas-phase organic acids and HNO_3 (a-h) and correlation between glutaric acid
 353 ($\text{C}_5\text{H}_8\text{O}_4$) and succinic acid ($\text{C}_4\text{H}_6\text{O}_4$) (i) from 19 buses after oxidation in the Go:PAM.

354
 355
 356



357 **3.2.3 Particulate emissions**

358 Table 3 displays the top 10 EFs of fresh particle-phase compounds (EF_{fresh}), as characterized by the FIGAERO ToF-CIMS,
 359 alongside their respective aged EFs (EF_{aged}), for Euro V DSL and RME buses. These top 10 EF_{fresh} contributed to over 82% of
 360 the total fresh particulate emissions measured by CIMS. Fresh particulate emissions from DSL buses were predominantly
 361 composed of sulfuric acid (H_2SO_4) and nitric acid (HNO_3). Benzene/toluene oxidation products ($C_7H_4O_7$, C_7H_8O , $C_6H_5NO_3$,
 362 C_6H_5O , $C_7H_7NO_3$) also had relatively high EF_{fresh} , aligning with the findings in Le Breton et al. (2019). Similarly, high EF_{fresh}
 363 of HNO_3 ($2.5 \text{ mg kg-fuel}^{-1}$) and H_2SO_4 ($0.61 \text{ kg-fuel}^{-1}$) were observed for the RME bus. Additionally, fatty acids, known as
 364 main components of unburned rapeseed oil (Usmanov et al., 2015), such as $C_{18}H_{34}O_2$, $C_{14}H_{28}O_2$, $C_{18}H_{36}O_2$, $C_{16}H_{32}O_2$, and
 365 $C_{16}H_{30}O_2$, significantly contributed to the identified mass loadings from the RME bus. When comparing the percentage mass
 366 observed by CIMS for both DSL and RME fuels in fresh and aged exhaust plumes, the total emission factors measured by
 367 CIMS (EF_{CIMS}) were notably lower than the total emission factors measured by the EEPS (EF_{total}). This difference is expected
 368 due to the sensitivity of the acetate ionization scheme of CIMS, which efficiently detects oxygenated volatile organic
 369 compounds, particularly carboxylic acids and inorganic acids, but has low sensitivity towards hydrocarbons and cannot detect
 370 metallic ions and soot. The CIMS measured EF_{fresh} accounted for 10.4% and 5.9% of the fresh EF_{total} measured by the EEPS
 371 for DSL and RME, respectively. In aged exhaust, EF_{CIMS} represented a higher percentage of EF_{total} (25.8% for DSL and 17.9%
 372 for RME), likely because of an increased proportion of organics with acid groups.

373

374 Table 3. Summary of top 10 EF_{fresh} of PM contributing species with respective EF_{aged} in Euro V DSL and RME emissions.

Species	DSL		Species	RME	
	EF_{fresh} ($\text{mg kg}_{\text{fuel}}^{-1}$)	EF_{aged} ($\text{mg kg}_{\text{fuel}}^{-1}$)		EF_{fresh} ($\text{mg kg}_{\text{fuel}}^{-1}$)	EF_{aged} ($\text{mg kg}_{\text{fuel}}^{-1}$)
H_2SO_4	4.8	6.8	HNO_3	2.5	45
HNO_3	3.2	50	$C_{18}H_{34}O_2$	1.2	0.81
$C_7H_4O_7$	1.8	3.8	H_2SO_4	0.61	0.68
$HNCO$	1.1	1.2	$C_{14}H_{28}O_2$	0.52	0.85
C_7H_8O	0.9	7.2	$HNCO$	0.45	0.089
$C_3H_6O_3$	0.6	23	$C_{18}H_{36}O_2$	0.32	0.046
$C_6H_5NO_3$	0.53	2.6	$C_{16}H_{32}O_2$	0.30	0.18
$C_4H_6O_5$	0.45	0.30	$C_6H_5O_2$	0.12	8.6
C_6H_5O	0.26	15.6	$C_4H_6O_4$	0.089	6.3
$C_7H_7NO_3$	0.15	4.6	$C_{16}H_{30}O_2$	0.081	0.012
EF_{total} measured by the EEPS	160.9	1289.8	EF_{total} measured by the EEPS	127.7	1320.6
EF_{CIMS}	16.8	320.1	EF_{CIMS}	7.5	237.2
$EF_{\text{CIMS}}/EF_{\text{total}}$ (%)	10.4	25.8	$EF_{\text{CIMS}}/EF_{\text{total}}$ (%)	5.9	17.9

375

376



377 4. Conclusion/ atmospheric implications

378 To address the challenges posed by increasing transportation needs, associated greenhouse gas emissions, and related climate
379 change impacts, biofuels have been promoted as a low-carbon alternative to fossil fuels. In 2020, for the 27 Member States of
380 the European Union, 93.2% of the total fuel supply for road transport was derived from fossil fuels, while 6.8% came from
381 biofuels, with Sweden having the highest biofuel share at 23.2% (Vourliotakis and Platsakis, 2022). This study investigated
382 renewable fuels like rapeseed methyl ester (RME), hydrotreated vegetable oil (HVO), and methane (when using biogas) in
383 terms of primary emissions of pollutants and their secondary formation after photochemical aging. DSL buses without a DPF
384 displayed the highest $EF_{PM:Fresh}$, whereas compressed natural gas (CNG) buses emitted the least, with a median $EF_{PM:Fresh}$ below
385 the detection limit. Despite more than an order of magnitude difference in $EF_{PM:Fresh}$ among buses operated using various fuel
386 types, secondary particle formation from the photooxidation of emissions was notable for all 76 buses studied. The median
387 ratio of aged to fresh particle mass emission factors, in ascending order, was diesel (4.0), HVO (6.7), HVO_{HEV} (10.5), RME
388 (10.8), and CNG buses (84). This underscores the importance of considering the potential for forming secondary particle mass
389 in future vehicle emission legislation and in evaluating environmental impacts. The omission of this secondary formation
390 process from current legislation, while important for climate and health reasons, can lead to an incomplete understanding of
391 the potential impact of mobile sources or emission control measures on regional air quality. The inclusion of secondary
392 pollutants in emission regulations is essential for a more comprehensive assessment of their effects.

393

394 Non-regulated chemical species can also have serious negative impacts on air quality and human health. Organic and inorganic
395 acids influence the pH of precipitation and will potentially contribute to acid deposition, affecting ecosystem health.
396 Furthermore, there is a risk that some abatement systems might generate specific compounds. For instance, isocyanic acid
397 (HNCO), a byproduct of urea- SCR exhaust systems, has been linked to health issues such as atherosclerosis, cataracts, and
398 rheumatoid arthritis (Leslie et al., 2019; Roberts et al., 2011). In our study, small monoacids (C₁-C₃) and nitrogen-containing
399 compounds, such as nitrous acid (HONO), nitric acid (HNO₃), and HNCO, dominated the fresh gaseous emissions measured
400 by acetate-CIMS for all Euro V/EEV buses regardless of fuel type, with HVO_{HEV} buses exhibiting the highest emissions.
401 Notably, nitrogen-containing compounds were significantly reduced in Euro VI buses, which operated with after-treatment
402 systems incorporating EGR and DPF in addition to SCR-only techniques. This indicates that transitioning to vehicles equipped
403 with more advanced emission control technologies can be beneficial, even though these technologies may not be specifically
404 designed to target emissions of HONO, HNO₃, and HNCO. Consequently, a detailed evaluation of the environmental and
405 health effects of emerging engine and after-treatment technologies is highly desirable for future considerations. Overall, the
406 extended online chemical characterization of in-use fleet emissions, utilizing advanced techniques like HR-ToF-CIMS, enables
407 the identification of unregulated pollutants, which is crucial for more informed policy decisions and vehicle technology
408 developments.

409



410 **Data availability.**

411 The data used in this publication are available to the community and can be accessed by request to the corresponding author.

412

413 **Author contributions.**

414 ÅMH, MLB and QL conducted the measurements. ÅMH designed the project, coordinated the measurements and together
415 with MH and CKC supervised the study. LZ, QL, MLB, CMS and ÅMH carried out the data analysis. LZ, QL, JZY, MH,
416 ÅMH and CKC prepared the manuscript. All co-authors contributed to the discussion and the interpretation of the results.

417

418 **Competing interests.**

419 The authors declare that they have no known competing financial interests or personal relationships that could have appeared
420 to influence the work reported in this paper.

421

422 **Acknowledgments.**

423 This work was financed by VINNOVA, Sweden's Innovation Agency (2013-03058) and Formas (2020-1907) and was an
424 initiative within the framework programme "Photochemical smog in China" financed by the Swedish Research Council (639-
425 2013-6917). Chak K. Chan would like to acknowledge the support of the National Natural Science Foundation of China
426 (project no. 41675117 and 41875142).

427 **References**

- 428 Aljawhary, D., Lee, A. K. Y., and Abbatt, J. P. D.: High-resolution chemical ionization mass spectrometry (ToF-CIMS): application to study
429 SOA composition and processing, *Atmospheric Measurement Techniques*, 6, 3211-3224, 10.5194/amt-6-3211-2013, 2013.
- 430 Bernhard, A. M., Peitz, D., Elsener, M., Wokaun, A., and Kröcher, O.: Hydrolysis and thermolysis of urea and its decomposition byproducts
431 biuret, cyanuric acid and melamine over anatase TiO₂, *Applied Catalysis B: Environmental*, 115, 129-137, 2012.
- 432 Bruns, E., El Haddad, I., Keller, A., Klein, F., Kumar, N., Pieber, S., Corbin, J., Slowik, J., Brune, W., and Baltensperger, U.: Inter-
433 comparison of laboratory smog chamber and flow reactor systems on organic aerosol yield and composition, *Atmospheric Measurement*
434 *Techniques*, 8, 2315-2332, 2015.
- 435 Chirico, R., DeCarlo, P., Heringa, M., Tritscher, T., Richter, R., Prévôt, A., Dommen, J., Weingartner, E., Wehrle, G., and Gysel, M.: Impact
436 of aftertreatment devices on primary emissions and secondary organic aerosol formation potential from in-use diesel vehicles: results from
437 smog chamber experiments, *Atmospheric Chemistry & Physics*, 10, 11545-11563, 2010.
- 438 Crisp, T. A., Brady, J. M., Cappa, C. D., Collier, S., Forestieri, S. D., Kleeman, M. J., Kuwayama, T., Lerner, B. M., Williams, E. J., and
439 Zhang, Q.: On the primary emission of formic acid from light duty gasoline vehicles and ocean-going vessels, *Atmospheric Environment*,
440 98, 426-433, 2014.
- 441 Deng, W., Hu, Q., Liu, T., Wang, X., Zhang, Y., Song, W., Sun, Y., Bi, X., Yu, J., Yang, W., Huang, X., Zhang, Z., Huang, Z., He, Q.,
442 Mellouki, A., and George, C.: Primary particulate emissions and secondary organic aerosol (SOA) formation from idling diesel vehicle
443 exhaust in China, *Sci Total Environ*, 593-594, 462-469, 10.1016/j.scitotenv.2017.03.088, 2017.
- 444 Edwards, R., Mahieu, V., Griesemann, J.-C., Larivé, J.-F., and Rickeard, D. J.: Well-to-wheels analysis of future automotive fuels and
445 powertrains in the European context, *SAE Technical Paper0148-7191*, 2004.
- 446 Energimyndigheten: *Energy in Sweden 2021 – An Overview*, 2021.
- 447 Fitzmaurice, H. L., and Cohen, R. C.: A method for using stationary networks to observe long-term trends of on-road emission factors of
448 primary aerosol from heavy-duty vehicles, *Atmospheric Chemistry and Physics*, 22, 15403-15411, 2022.
- 449 Friedman, B., Link, M. F., Fulgham, S. R., Brophy, P., Galang, A., Brune, W. H., Jathar, S. H., and Farmer, D. K.: Primary and Secondary
450 Sources of Gas-Phase Organic Acids from Diesel Exhaust, *Environ Sci Technol*, 51, 10872-10880, 10.1021/acs.est.7b01169, 2017.



- 451 Gentner, D. R., Jathar, S. H., Gordon, T. D., Bahreini, R., Day, D. A., El Haddad, I., Hayes, P. L., Pieber, S. M., Platt, S. M., and de Gouw,
452 J.: Review of urban secondary organic aerosol formation from gasoline and diesel motor vehicle emissions, *Environmental science &*
453 *technology*, 51, 1074-1093, 2017.
- 454 Ghadimi, S., Zhu, H., Durbin, T. D., Cocker III, D. R., and Karavalakis, G.: Exceedances of Secondary Aerosol Formation from In-Use
455 Natural Gas Heavy-Duty Vehicles Compared to Diesel Heavy-Duty Vehicles, *Environmental Science & Technology*, 57, 19979-19989,
456 2023.
- 457 Gordon, T. D., Presto, A. A., May, A. A., Nguyen, N. T., Lipsky, E. M., Donahue, N. M., Gutierrez, A., Zhang, M., Maddox, C., Rieger, P.,
458 Chattopadhyay, S., Maldonado, H., Maricq, M. M., and Robinson, A. L.: Secondary organic aerosol formation exceeds primary particulate
459 matter emissions for light-duty gasoline vehicles, *Atmospheric Chemistry and Physics*, 14, 4661-4678, 10.5194/acp-14-4661-2014, 2014a.
- 460 Gordon, T. D., Presto, A. A., Nguyen, N. T., Robertson, W. H., Na, K., Sahay, K. N., Zhang, M., Maddox, C., Rieger, P., Chattopadhyay,
461 S., Maldonado, H., Maricq, M. M., and Robinson, A. L.: Secondary organic aerosol production from diesel vehicle exhaust: impact of
462 aftertreatment, fuel chemistry and driving cycle, *Atmospheric Chemistry and Physics*, 14, 4643-4659, 10.5194/acp-14-4643-2014, 2014b.
- 463 Guerreiro, C. B., Foltescu, V., and De Leeuw, F.: Air quality status and trends in Europe, *Atmospheric environment*, 98, 376-384, 2014.
- 464 Hak, C. S., Hallquist, M., Ljungstrom, E., Svane, M., and Pettersson, J. B. C.: A new approach to in-situ determination of roadside particle
465 emission factors of individual vehicles under conventional driving conditions, *Atmospheric Environment*, 43, 2481-2488,
466 10.1016/j.atmosenv.2009.01.041, 2009.
- 467 Hallquist, A. M., Jerksjo, M., Fallgren, H., Westerlund, J., and Sjodin, A.: Particle and gaseous emissions from individual diesel and CNG
468 buses, *Atmospheric Chemistry and Physics*, 13, 5337-5350, 10.5194/acp-13-5337-2013, 2013.
- 469 Hallquist, M., Wenger, J. C., Baltensperger, U., Rudich, Y., Simpson, D., Claeys, M., Dommen, J., Donahue, N., George, C., and Goldstein,
470 A.: The formation, properties and impact of secondary organic aerosol: current and emerging issues, *Atmospheric chemistry and physics*, 9,
471 5155-5236, 2009.
- 472 Hassaneen, A., Munack, A., Ruschel, Y., Schroeder, O., and Krahl, J.: Fuel economy and emission characteristics of Gas-to-Liquid (GTL)
473 and Rapeseed Methyl Ester (RME) as alternative fuels for diesel engines, *Fuel*, 97, 125-130, 2012.
- 474 Janhäll, S., and Hallquist, M.: A novel method for determination of size-resolved, submicrometer particle traffic emission factors,
475 *Environmental Science & Technology*, 39, 7609-7615, <http://doi.org/10.1021/es048208y>, 2005.
- 476 Jathar, S. H., Friedman, B., Galang, A. A., Link, M. F., Brophy, P., Volckens, J., Eluri, S., and Farmer, D. K.: Linking load, fuel, and
477 emission controls to photochemical production of secondary organic aerosol from a diesel engine, *Environmental science & technology*, 51,
478 1377-1386, 2017a.
- 479 Jathar, S. H., Heppding, C., Link, M. F., Farmer, D. K., Akherati, A., Kleeman, M. J., de Gouw, J. A., Veres, P. R., and Roberts, J. M.:
480 Investigating diesel engines as an atmospheric source of isocyanic acid in urban areas, *Atmospheric Chemistry and Physics*, 17, 8959-8970,
481 10.5194/acp-17-8959-2017, 2017b.
- 482 Jezek, I., Drinovec, L., Ferrero, L., Carriero, M., and Mocnik, G.: Determination of car on-road black carbon and particle number emission
483 factors and comparison between mobile and stationary measurements, *Atmospheric Measurement Techniques*, 8, 43-55, 10.5194/amt-8-43-
484 2015, 2015.
- 485 Kang, E., Root, M. J., Toohey, D. W., and Brune, W. H.: Introducing the concept of Potential Aerosol Mass (PAM), *Atmospheric Chemistry*
486 *and Physics*, 7, 5727-5744, DOI 10.5194/acp-7-5727-2007, 2007.
- 487 Kroll, J. H., Smith, J. D., Che, D. L., Kessler, S. H., Worsnop, D. R., and Wilson, K. R.: Measurement of fragmentation and functionalization
488 pathways in the heterogeneous oxidation of oxidized organic aerosol, *Physical Chemistry Chemical Physics*, 11, 8005-8014, 2009.
- 489 Kuitinen, N., McCaffery, C., Peng, W., Zimmermann, S., Roth, P., Simonen, P., Karjalainen, P., Keskinen, J., Cocker, D. R., and Durbin, T.
490 D.: Effects of driving conditions on secondary aerosol formation from a GDI vehicle using an oxidation flow reactor, *Environmental*
491 *Pollution*, 282, 117069, 2021.
- 492 Kurtenbach, R., Becker, K., Gomes, J., Kleffmann, J., Lörzer, J., Spittler, M., Wiesen, P., Ackermann, R., Geyer, A., and Platt, U.:
493 Investigations of emissions and heterogeneous formation of HONO in a road traffic tunnel, *Atmospheric Environment*, 35, 3385-3394, 2001.
- 494 Kwak, J. H., Kim, H. S., Lee, J. H., and Lee, S. H.: On-Road Chasing Measurement of Exhaust Particle Emissions from Diesel, Cng Lpg
495 and Dme-Fueled Vehicles Using a Mobile Emission Laboratory, *International Journal of Automotive Technology*, 15, 543-551,
496 <http://doi.org/10.1007/s12239-014-0057-z>, 2014.
- 497 Lambe, A., Ahern, A., Williams, L., Slowik, J., Wong, J., Abbatt, J., Brune, W., Ng, N., Wright, J., and Croasdale, D.: Characterization of
498 aerosol photooxidation flow reactors: heterogeneous oxidation, secondary organic aerosol formation and cloud condensation nuclei activity
499 measurements, *Atmospheric Measurement Techniques*, 4, 445-461, 2011.
- 500 Le Breton, M., Wang, Y., Hallquist, Å. M., Pathak, R. K., Zheng, J., Yang, Y., Shang, D., Glasius, M., Bannan, T. J., and Liu, Q.: Online
501 gas-and particle-phase measurements of organosulfates, organosulfonates and nitrooxy organosulfates in Beijing utilizing a FIGAERO ToF-
502 CIMS, *Atmospheric Chemistry and Physics*, 18, 10355-10371, 2018.
- 503 Le Breton, M., Psichoudaki, M., Hallquist, M., Watne, Å., Lutz, A., and Hallquist, Å.: Application of a FIGAERO ToF CIMS for on-line
504 characterization of real-world fresh and aged particle emissions from buses, *Aerosol Science and Technology*, 53, 244-259, 2019.
- 505 Leslie, M. D., Ridoli, M., Murphy, J. G., and Borduas-Dedekind, N.: Isocyanic acid (HNCO) and its fate in the atmosphere: a review,
506 *Environmental Science: Processes & Impacts*, 21, 793-808, 2019.



- 507 Li, T., Wang, Z., Yuan, B., Ye, C., Lin, Y., Wang, S., Yuan, Z., Zheng, J., and Shao, M.: Emissions of carboxylic acids, hydrogen cyanide
508 (HCN) and isocyanic acid (HNCO) from vehicle exhaust, *Atmospheric Environment*, 247, 118218, 2021.
- 509 Liao, K., Chen, Q., Liu, Y., Li, Y. J., Lambe, A. T., Zhu, T., Huang, R.-J., Zheng, Y., Cheng, X., and Miao, R.: Secondary organic aerosol
510 formation of fleet vehicle emissions in China: Potential seasonality of spatial distributions, *Environmental Science & Technology*, 55, 7276-
511 7286, 2021.
- 512 Liao, S., Zhang, J., Yu, F., Zhu, M., Liu, J., Ou, J., Dong, H., Sha, Q., Zhong, Z., and Xie, Y.: High gaseous nitrous acid (HONO) emissions
513 from light-duty diesel vehicles, *Environmental science & technology*, 55, 200-208, 2020.
- 514 Liu, Q., Hallquist, Å. M., Fallgren, H., Jerksjö, M., Jutterström, S., Salberg, H., Hallquist, M., Le Breton, M., Pei, X., and Pathak, R. K.:
515 Roadside assessment of a modern city bus fleet: Gaseous and particle emissions, *Atmospheric Environment: X*, 3, 100044, 2019a.
- 516 Liu, S., Thompson, S. L., Stark, H., Ziemann, P. J., and Jimenez, J. L.: Gas-phase carboxylic acids in a university classroom: Abundance,
517 variability, and sources, *Environmental Science & Technology*, 51, 5454-5463, 2017.
- 518 Liu, T., Wang, X., Deng, W., Hu, Q., Ding, X., Zhang, Y., He, Q., Zhang, Z., Lu, S., Bi, X., Chen, J., and Yu, J.: Secondary organic aerosol
519 formation from photochemical aging of light-duty gasoline vehicle exhausts in a smog chamber, *Atmospheric Chemistry and Physics*, 15,
520 9049-9062, 10.5194/acp-15-9049-2015, 2015.
- 521 Liu, T., Zhou, L., Liu, Q., Lee, B. P., Yao, D., Lu, H., Lyu, X., Guo, H., and Chan, C. K.: Secondary Organic Aerosol Formation from Urban
522 Roadside Air in Hong Kong, *Environ Sci Technol*, 53, 3001-3009, 10.1021/acs.est.8b06587, 2019b.
- 523 Lopez-Hilfiker, F., Mohr, C., Ehn, M., Rubach, F., Kleist, E., Wildt, J., Mentel, T. F., Carrasquillo, A., Daumit, K., and Hunter, J.: Phase
524 partitioning and volatility of secondary organic aerosol components formed from α -pinene ozonolysis and OH oxidation: the importance of
525 accretion products and other low volatility compounds, *Atmospheric chemistry and physics*, 15, 7765-7776, 2015.
- 526 Lopez-Hilfiker, F. D., Mohr, C., Ehn, M., Rubach, F., Kleist, E., Wildt, J., Mentel, T. F., Lutz, A., Hallquist, M., Worsnop, D., and Thornton,
527 J. A.: A novel method for online analysis of gas and particle composition: description and evaluation of a Filter Inlet for Gases and AEROSols
528 (FIGAERO), *Atmospheric Measurement Techniques*, 7, 983-1001, 10.5194/amt-7-983-2014, 2014.
- 529 Martinet, S., Liu, Y., Louis, C., Tassel, P., Perret, P., Chaumond, A., and Andre, M.: Euro 6 unregulated pollutant characterization and
530 statistical analysis of after-treatment device and driving-condition impact on recent passenger-car emissions, *Environmental Science &
531 Technology*, 51, 5847-5855, 2017.
- 532 May, A. A., Nguyen, N. T., Presto, A. A., Gordon, T. D., Lipsky, E. M., Karve, M., Gutierrez, A., Robertson, W. H., Zhang, M., Brandow,
533 C., Chang, O., Chen, S. Y., Cicero-Fernandez, P., Dinkins, L., Fuentes, M., Huang, S. M., Ling, R., Long, J., Maddox, C., Massetti, J.,
534 McCauley, E., Miguel, A., Na, K., Ong, R., Pang, Y. B., Rieger, P., Sax, T., Truong, T., Vo, T., Chattopadhyay, S., Maldonado, H., Maricq,
535 M. M., and Robinson, A. L.: Gas- and particle-phase primary emissions from in-use, on-road gasoline and diesel vehicles, *Atmospheric
536 Environment*, 88, 247-260, 10.1016/j.atmosenv.2014.01.046, 2014.
- 537 Millet, D. B., Baasandorj, M., Farmer, D. K., Thornton, J. A., Baumann, K., Brophy, P., Chaliyakunnel, S., de Gouw, J. A., Graus, M., and
538 Hu, L.: A large and ubiquitous source of atmospheric formic acid, *Atmospheric Chemistry and Physics*, 15, 6283-6304, 2015.
- 539 Mohr, C., Lopez-Hilfiker, F. D., Yli-Juuti, T., Heitto, A., Lutz, A., Hallquist, M., D'Ambro, E. L., Rissanen, M. P., Hao, L., and
540 Schobesberger, S.: Ambient observations of dimers from terpene oxidation in the gas phase: Implications for new particle formation and
541 growth, *Geophysical Research Letters*, 44, 2958-2966, 2017.
- 542 Nakashima, Y., and Kondo, Y.: Nitrous acid (HONO) emission factors for diesel vehicles determined using a chassis dynamometer, *Science
543 of The Total Environment*, 806, 150927, 2022.
- 544 Nordin, E. Z., Eriksson, A. C., Roldin, P., Nilsson, P. T., Carlsson, J. E., Kajos, M. K., Hellen, H., Wittbom, C., Rissler, J., Londahl, J.,
545 Swietlicki, E., Svenningsson, B., Bohgard, M., Kulmala, M., Hallquist, M., and Pagels, J. H.: Secondary organic aerosol formation from
546 idling gasoline passenger vehicle emissions investigated in a smog chamber, *Atmospheric Chemistry and Physics*, 13, 6101-6116,
547 10.5194/acp-13-6101-2013, 2013.
- 548 Ortega, A. M., Hayes, P. L., Peng, Z., Palm, B. B., Hu, W., Day, D. A., Li, R., Cubison, M. J., Brune, W. H., and Graus, M.: Real-time
549 measurements of secondary organic aerosol formation and aging from ambient air in an oxidation flow reactor in the Los Angeles area,
550 *Atmospheric Chemistry and Physics*, 16, 7411-7433, 2016.
- 551 Palm, B. B., Campuzano-Jost, P., Ortega, A. M., Day, D. A., Kaser, L., Jud, W., Karl, T., Hansel, A., Hunter, J. F., and Cross, E. S.: In situ
552 secondary organic aerosol formation from ambient pine forest air using an oxidation flow reactor, *Atmospheric Chemistry and Physics*, 16,
553 2943-2970, 2016.
- 554 Paulot, F., Wunch, D., Crouse, J. D., Toon, G., Millet, D. B., DeCarlo, P. F., Vigouroux, C., Deutscher, N. M., González Abad, G., and
555 Notholt, J.: Importance of secondary sources in the atmospheric budgets of formic and acetic acids, *Atmospheric Chemistry and Physics*,
556 11, 1989-2013, 2011.
- 557 Pflaum, H., Hofmann, P., Geringer, B., and Weissel, W.: Potential of hydrogenated vegetable oil (HVO) in a modern diesel engine, *SAE
558 Technical Paper0148-7191*, 2010.
- 559 Pirjola, L., Dittrich, A., Niemi, J. V., Saarikoski, S., Timonen, H., Kuuluvainen, H., Jarvinen, A., Kousa, A., Ronkko, T., and Hillamo, R.:
560 Physical and Chemical Characterization of Real-World Particle Number and Mass Emissions from City Buses in Finland, *Environ Sci
561 Technol*, 50, 294-304, <http://doi.org/10.1021/acs.est.5b04105>, 2016.



- 562 Platt, S. M., El Haddad, I., Zardini, A. A., Clairotte, M., Astorga, C., Wolf, R., Slowik, J. G., Temime-Roussel, B., Marchand, N., Jezek, I.,
563 Drinovec, L., Mocnik, G., Mohler, O., Richter, R., Barmet, P., Bianchi, F., Baltensperger, U., and Prevot, A. S. H.: Secondary organic aerosol
564 formation from gasoline vehicle emissions in a new mobile environmental reaction chamber, *Atmospheric Chemistry and Physics*, 13, 9141-
565 9158, 10.5194/acp-13-9141-2013, 2013.
- 566 Preble, C. V., Dallmann, T. R., Kreisberg, N. M., Hering, S. V., Harley, R. A., and Kirchstetter, T. W.: Effects of Particle Filters and Selective
567 Catalytic Reduction on Heavy-Duty Diesel Drayage Truck Emissions at the Port of Oakland, *Environmental Science & Technology*, 49,
568 8864-8871, 10.1021/acs.est.5b01117, 2015.
- 569 Roberts, J. M., Veres, P. R., Cochran, A. K., Warneke, C., Burling, I. R., Yokelson, R. J., Lerner, B., Gilman, J. B., Kuster, W. C., and Fall,
570 R.: Isocyanic acid in the atmosphere and its possible link to smoke-related health effects, *Proceedings of the National Academy of Sciences*,
571 108, 8966-8971, 2011.
- 572 Saliba, G., Saleh, R., Zhao, Y., Presto, A. A., Lambe, A. T., Frodin, B., Sardar, S., Maldonado, H., Maddox, C., and May, A. A.: Comparison
573 of gasoline direct-injection (GDI) and port fuel injection (PFI) vehicle emissions: emission certification standards, cold-start, secondary
574 organic aerosol formation potential, and potential climate impacts, *Environmental science & technology*, 51, 6542-6552, 2017.
- 575 Simonen, P., Saukko, E., Karjalainen, P., Timonen, H., Bloss, M., Aakko-Saksa, P., Rönkkö, T., Keskinen, J., and Dal Maso, M.: A new
576 oxidation flow reactor for measuring secondary aerosol formation of rapidly changing emission sources, *Atmospheric Measurement
577 Techniques*, 10, 1519-1537, 2017.
- 578 Suarez-Bertoa, R., and Astorga, C.: Isocyanic acid and ammonia in vehicle emissions, *Transportation Research Part D: Transport and
579 Environment*, 49, 259-270, 2016.
- 580 Tkacik, D. S., Lambe, A. T., Jathar, S., Li, X., Presto, A. A., Zhao, Y. L., Blake, D., Meinardi, S., Jayne, J. T., Croteau, P. L., and Robinson,
581 A. L.: Secondary Organic Aerosol Formation from in-Use Motor Vehicle Emissions Using a Potential Aerosol Mass Reactor, *Environmental
582 Science & Technology*, 48, 11235-11242, 10.1021/es502239v, 2014.
- 583 Usmanov, R. A., Mazanov, S. V., Gabitova, A. R., Miftakhova, L. K., Gumerov, F. M., Musin, R. Z., and Abdulagatov, I. M.: The effect of
584 fatty acid ethyl esters concentration on the kinematic viscosity of biodiesel fuel, *Journal of Chemical & Engineering Data*, 60, 3404-3413,
585 2015.
- 586 Vourliotakis, G., and Platsakis, O.: ETC CM report 2022/02: Greenhouse gas intensities of transport fuels in the EU in 2020 - Monitoring
587 under the Fuel Quality Directive, European Topic Centre on Climate change mitigation, 2022.
- 588 Watne, A. K., Psichoudaki, M., Ljungstrom, E., Le Breton, M., Hallquist, M., Jerksjo, M., Fallgren, H., Jutterstrom, S., and Hallquist, A.
589 M.: Fresh and Oxidized Emissions from In-Use Transit Buses Running on Diesel, Biodiesel, and CNG, *Environ Sci Technol*, 52, 7720-7728,
590 <https://doi.org/10.1021/acs.est.8b01394>, 2018.
- 591 Wentzell, J. J., Liggio, J., Li, S. M., Vlasenko, A., Staebler, R., Lu, G., Poitras, M. J., Chan, T., and Brook, J. R.: Measurements of gas phase
592 acids in diesel exhaust: a relevant source of HNC₂O?, *Environ Sci Technol*, 47, 7663-7671, 10.1021/es401127j, 2013.
- 593 Yao, D., Guo, H., Lyu, X., Lu, H., and Huo, Y.: Secondary organic aerosol formation at an urban background site on the coastline of South
594 China: Precursors and aging processes, *Environmental Pollution*, 309, 119778, 2022.
- 595 Yao, X., Fang, M., and Chan, C. K.: Size distributions and formation of dicarboxylic acids in atmospheric particles, *Atmospheric
596 Environment*, 36, 2099-2107, 2002.
- 597 Yuan, B., Veres, P., Warneke, C., Roberts, J., Gilman, J., Koss, A., Edwards, P., Graus, M., Kuster, W., and Li, S.-M.: Investigation of
598 secondary formation of formic acid: urban environment vs. oil and gas producing region, *Atmospheric Chemistry and Physics*, 15, 1975-
599 1993, 2015.
- 600 Zhao, Y., Lambe, A. T., Saleh, R., Saliba, G., and Robinson, A. L.: Secondary Organic Aerosol Production from Gasoline Vehicle Exhaust:
601 Effects of Engine Technology, Cold Start, and Emission Certification Standard, *Environ Sci Technol*, 52, 1253-1261,
602 <https://doi.org/10.1021/acs.est.7b05045>, 2018.
- 603 Zhou, L., Hallquist, Å. M., Hallquist, M., Salvador, C. M., Gaita, S. M., Sjödin, Å., Jerksjö, M., Salberg, H., Wängberg, I., and Mellqvist,
604 J.: A transition of atmospheric emissions of particles and gases from on-road heavy-duty trucks, *Atmospheric Chemistry and Physics*, 20,
605 1701-1722, 2020.
- 606 Zhou, L., Salvador, C. M., Priestley, M., Hallquist, M., Liu, Q., Chan, C. K., and Hallquist, Å. M.: Emissions and secondary formation of
607 air pollutants from modern heavy-duty trucks in real-world traffic—chemical characteristics using on-line mass spectrometry, *Environmental
608 Science & Technology*, 55, 14515-14525, 2021.
- 609